Available online at www.sciencedirect.com
ScienceDirect
Journal of Sound and Vibration 320 (2009) 235–253
JOURNAL OF SOUND AND VIBRATION
www.elsevier.com/locate/jsvi

Nonlinear dynamic analysis of an eccentrically prestressed damped beam under a concentrated moving harmonic load

M. Şimşek*, T. Kocatürk

Department of Civil Engineering, Yildiz Technical University, Yildiz 34349, İstanbul, Turkey

Received 2 August 2007; received in revised form 16 July 2008; accepted 21 July 2008
Handling Editor: A.V. Metrikine
Available online 3 September 2008

Abstract

This paper focuses on the geometrically nonlinear dynamic analysis of an eccentrically prestressed simply supported damped beam subjected to a concentrated moving harmonic load. The nonlinear dynamic deflections of the beam are obtained by polynomial functions. The Kelvin–Voigt model for the material of the beam is used. Two coupled nonlinear systems of equations of motion are derived using Lagrange's equations under the assumptions of the Euler–Bernoulli beam theory with the von-Kármán's nonlinear strain–displacement relationships. The rotary inertia, axial displacement and axial inertia are included in the formulation. The nonlinear equations of motion are solved by using the implicit time integration method of Newmark-β in conjunction with the Newton–Raphson iteration method. In this study, the effects of large deflections, the internal damping of the beam, the velocity of the moving harmonic load, the prestress load, the eccentricity of the prestress load and the excitation frequency on the dynamic response of the beam are discussed. The obtained results are compared with the results based on the linear beam theory. Convergence studies are performed. Numerical results show that the above-mentioned effects play a very important role in the deflections of the beam.

1. Introduction

Linear and nonlinear free and forced vibrations of structural elements, such as beams and plates, have been studied extensively. When beams (or plates) are subjected to loads with large magnitude or to harmonic loads whose frequency is close to natural frequency of the beam, the beam may vibrate with large amplitude. For this reason, the linear beam theory (small deflection theory) may give erroneous results so that it must be extended to include the effects of the large deflection. Although beams subjected to moving loads have been widely studied according to the linear beam theory (see Refs. [1–19]), the research effort devoted to nonlinear vibration of beams under the moving loads has been limited. For example, Hino et al. [20] analyzed the nonlinear vibrations of variable cross-sectional beams subjected to a moving load using the Galerkin finite element method. Yoshimura et al. [21] presented the analysis of dynamic deflections of a beam, including the effects of geometric nonlinearity, using the Galerkin method, a form of the method of weighted residuals.

*Corresponding author. Tel.: +90 2123832921; fax: +90 2122596762.
E-mail address: mesutsimsek@gmail.com (M. Şimşek).

0022-460X/$ - see front matter © 2008 Elsevier Ltd. All rights reserved.
doi:10.1016/j.jsv.2008.07.012

Nomenclature

$a_0,\ldots,a_7$	parameters in Newmark's method
A	area of the cross-section
A_n	time-dependent generalized coordinate of the transverse displacements
b_0,b_1,b_2	parameters in the Kelvin–Voigt model
b	width of the cross-section
B_n	time-dependent generalized coordinate of the axial displacements
$c(t)$	unit step function
c_b	a coefficient of the internal damping of the beam
$\mathbf{C}$	damping matrix
D	dissipation function
e	eccentricity of the prestress load
E	Young's modulus
$\mathbf{f}(t)$	generalized load vector
$\hat{\mathbf{F}}$	effective load vector
h	depth of the cross-section
I	moment of inertia of the cross-section
J	functional of the problem
J^*	Lagrangian functional of the problem
K_e	kinetic energy of the beam
$\mathbf{K}^L$	linear stiffness matrix
$\mathbf{K}_6^S,\ldots,\mathbf{K}_9^S$	matrices due to Lagrange multipliers
$\mathbf{K}^{NL}$	nonlinear stiffness matrix
$\hat{\mathbf{K}}$	effective stiffness matrix
$\hat{\mathbf{K}}_T$	tangent stiffness matrix
L	length of the beam
$\mathbf{M}$	mass matrix of the beam
M_b	bending moment
M_T	couple due to the eccentricity of prestress load
N	number of terms in the displacement functions
N_x	internal normal force
$P(t)$	moving harmonic load
P_0	amplitude of the moving harmonic load
$\mathbf{q}(t)$	generalized coordinates
Q_D	generalized damping force
$\mathbf{R}$	residual vector
s	iteration number
t	time
t_1	time the load $P(t)$ comes onto the beam
t_2	time the load $P(t)$ leaves the beam
T	eccentric prestress load
T_{cr}	Euler's buckling load
u	axial displacement
u_0	axial displacement of any point on the neutral axis
U	strain energy of the beam
v	velocity of the moving harmonic load
V	potential of the external loads
w	transverse displacement
w_0	transverse displacement of any point on the neutral axis
x	x coordinate
x_P	location of the moving harmonic load
z	z coordinate

Greek letters

α,δ	parameters in Newmark's method
β_1,β_2,β_3	Lagrange multipliers
ε_x	normal strain
ζ_{tol}	tolerance criterion
η	proportionality constant of the damping
ρ	mass of the beam per unit volume
σ_x	normal stress
ω_{1l}	the first linear natural frequency
Ω	excitation frequency of the moving harmonic load

Yoshimura et al. [22] used the finite element method to investigate the random nonlinear vibration analysis of variable cross-sectional beams subjected to a moving load. Chang and Liu [23] performed the deterministic and random vibration analysis of a nonlinear beam on an elastic foundation subjected to a moving load by the finite element method. Xu et al. [24] studied the transverse and longitudinal motions of a finite elastic beam traversed by a moving mass using Hamilton's principle. In Ref. [24], the obtained two nonlinear coupled differential equations governing the longitudinal and transverse displacements were solved by a finite difference method combined with a perturbation technique. Wang and Chou [25] adopted the large deflection theory to study the nonlinear vibration of the Timoshenko beam caused by the coupling effect of a moving force with the weight of the beam. Yanmeni et al. [26] investigated the nonlinear dynamics of a beam under moving loads using the multiple scales method. In Ref. [26], attention is paid to nonlinearity, which may be caused by large curvatures or nonlinear stretching of the mid-plane of the beam.

Pre-tensioning or post-tensioning is widely used in civil engineering applications, such as prestressed beams of viaducts of roadways, railways and bridges. Prestressing involves the application of an initial compressive load on a structure to reduce or eliminate the internal tensile stresses that may be caused by imposed loads or deformations, or by load-independent effects such as temperature changes or shrinkage. To the best of the authors' knowledge, this is the first attempt on the geometrically nonlinear vibration of an eccentrically prestressed damped beam subjected to a moving harmonic load. In the studies [20–26] on geometrically nonlinear beams mentioned above, there is no prestress load and the moving load is not harmonic, namely it is a constant moving load.

The aim of this paper is to investigate the geometrically nonlinear vibration of an eccentrically prestressed damped beam subjected to a concentrated moving harmonic load. In this study, von-Kármán's nonlinear strain–displacement relationships are used. The externally applied eccentric prestressed load is resolved into an axial prestressed load and a couple at the center of the cross-section of the beam. The nonlinear dynamic responses of the beam are obtained by the polynomial functions. The Kelvin–Voigt model for the material of the beam is used. Two coupled nonlinear systems of equations of motion are derived by using Lagrange's equations under the assumptions of the Euler–Bernoulli beam theory. Rotary inertia, axial displacement and axial inertia are included in the formulation. The equations of motion are solved by using the implicit time integration method of Newmark-β [28] in conjunction with the Newton–Raphson method, and then displacements, velocities and accelerations of the beam at the considered point and time are determined. Convergence studies are performed for various number of the term in the displacement functions, and for the different time steps. The obtained nonlinear results are compared with the results based on the linear beam theory.

2. Theory and formulations

An eccentrically prestressed simply supported isotropic beam of length L, width b, depth h, with the coordinate system (O; x, y, z) having the origin O is shown in Fig. 1. The beam is subjected to the externally applied eccentric prestress load, T, and the concentrated moving harmonic load, $P(t)$, which moves in the axial direction of the beam with constant velocity.

The canonical form of the Kelvin–Voigt model and its special case, which is used in the present study, can be expressed as follows:

$$b_0\sigma_x = b_1\varepsilon_x + b_2\dot{\varepsilon}_x;\ b_0 = 1,\ b_1 = E,\ b_2 = c_b = E\eta \tag{1a}$$

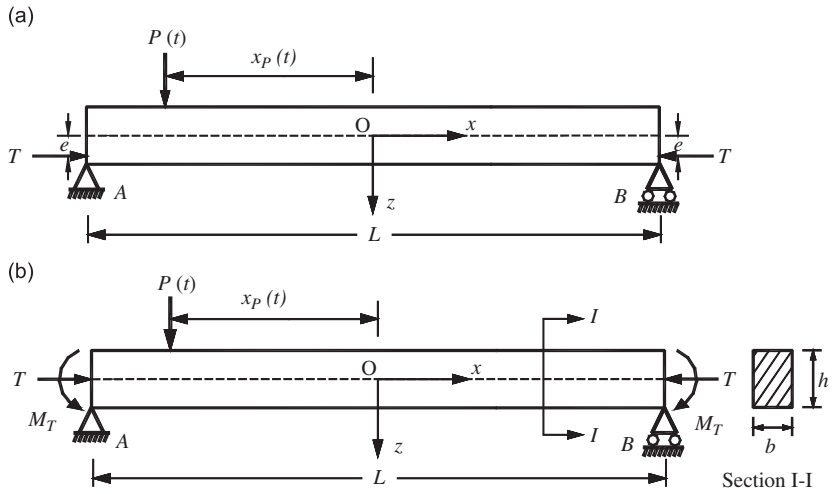

Fig. 1. (a) An eccentrically prestressed simply supported beam subjected to a moving harmonic load, (b) transferring the eccentric compressive load to the center of the cross-section of the beam as a compressive axial load and a couple.

$$\sigma_x = \sigma_x^e + \sigma_x^d = E\varepsilon_x + c_b\dot{\varepsilon}_x = E(\varepsilon_x + \eta\dot{\varepsilon}_x) \tag{1b}$$

where $(\dot{})$ indicates the derivative with respect to time, σ_x is the normal stress, E Young's modulus, c_b the coefficient of the internal damping of the beam and η the proportionality constant of the internal damping of the beam. Dimensions of the coefficient of the internal damping of the beam and proportionality constant of the internal damping of the beam are $\mathrm{N\,s/m^2}$ and s, respectively.

Based on the Euler–Bernoulli beam theory, the axial displacement, u, and the transverse displacement of any point of the beam, w, are given by

$$u(x,z,t) = u_0(x,t) - z\frac{\partial w_0(x,t)}{\partial x} \tag{2a}$$

$$w(x,z,t) = w_0(x,t) \tag{2b}$$

where u_0 and w_0 are the axial and the transverse displacement of any point on the neutral axis, z is the distance of any point from the neutral axis, t denotes time. The von-Kármán's nonlinear strain–displacement relationships based on assumptions of large transverse displacements, moderate rotations and small strains for a straight beam are given below:

$$\varepsilon_x = \frac{\partial u_0(x,t)}{\partial x} + \frac{1}{2}\left(\frac{\partial w_0(x,t)}{\partial x}\right)^2 - z\frac{\partial^2 w_0(x,t)}{\partial x^2} \tag{3a}$$

$$\dot{\varepsilon}_x = \frac{\partial \dot{u}_0(x,t)}{\partial x} + \left(\frac{\partial w_0(x,t)}{\partial x}\right)\left(\frac{\partial \dot{w}_0(x,t)}{\partial x}\right) - z\frac{\partial^2 \dot{w}_0(x,t)}{\partial x^2} \tag{3b}$$

where ε_x and $\dot{\varepsilon}_x$ are the normal strain and normal strain rate, respectively. Using Eqs. (1) and (3), the Euler–Bernoulli beam theory that normal stresses and strains vary linearly over the cross-section of the beam leads to the relations

$$M_b = -EI\frac{\partial^2 w_0(x,t)}{\partial x^2} - \eta EI\frac{\partial^2 \dot{w}_0(x,t)}{\partial x^2} \tag{4a}$$

$$N_x = EA\left[\frac{\partial u_0(x,t)}{\partial x} + \frac{1}{2}\left(\frac{\partial w_0(x,t)}{\partial x}\right)^2\right] + \eta EA\left[\frac{\partial \dot{u}_0(x,t)}{\partial x} + \left(\frac{\partial w_0(x,t)}{\partial x}\right)\left(\frac{\partial \dot{w}_0(x,t)}{\partial x}\right)\right] \tag{4b}$$

where M_b is the bending moment, N_x the internal normal force, I the moment of inertia of the cross-section of the beam, A the area of the cross-section of the beam. According to the Euler–Bernoulli beam theory, the strain energy of the beam, U, at any instant is

$$U = \frac{1}{2}\int_{-L/2}^{L/2}\int_A \sigma_x^e\varepsilon_x \,\mathrm{d}A\,\mathrm{d}x \tag{5}$$

With the help of Eqs. (1) and (3a), the strain energy of the beam at any instant can be expressed as

$$U = \frac{1}{2}\int_{-L/2}^{L/2}\left\{EA\left[\frac{\partial u_0(x,t)}{\partial x} + \frac{1}{2}\left(\frac{\partial w_0(x,t)}{\partial x}\right)^2\right]^2 + EI\left(\frac{\partial^2 w_0(x,t)}{\partial x^2}\right)^2\right\}\mathrm{d}x \tag{6}$$

The dissipation function of the beam, D, at any instant is given below

$$D = \frac{1}{2}\int_{-L/2}^{L/2}\int_A \sigma_x^d\dot{\varepsilon}_x \mathrm{d}A\,\mathrm{d}x \tag{7}$$

Likewise, the dissipation function of the beam at any instant can be obtained as follows:

$$D=\frac{1}{2}\int_{-L/2}^{L/2}\left\{\left[\eta EA\left(\frac{\partial\dot{u}_0(x,t)}{\partial x}\right)^2+\eta EI\left(\frac{\partial^2\dot{w}_0(x,t)}{\partial x^2}\right)^2\right]\right.$$
$$\left.+\eta EA\left[\left(\frac{\partial w_0(x,t)}{\partial x}\right)\left(\frac{\partial\dot{w}_0(x,t)}{\partial x}\right)\right]^2+2\eta EA\left(\frac{\partial\dot{u}_0(x,t)}{\partial x}\right)\left(\frac{\partial w_0(x,t)}{\partial x}\right)\left(\frac{\partial\dot{w}_0(x,t)}{\partial x}\right)\right\}\mathrm{d}x \tag{8}$$

The last two terms are very small compared with the first two terms in Eq. (8), and they are neglected. In this case, Eq. (8) becomes as follows:

$$D=\frac{1}{2}\int_{-L/2}^{L/2}\left[\eta EA\left(\frac{\partial\dot{u}_0(x,t)}{\partial x}\right)^2+\eta EI\left(\frac{\partial^2\dot{w}_0(x,t)}{\partial x^2}\right)^2\right]\mathrm{d}x \tag{9}$$

Including the rotary inertia and the axial inertia effects, the kinetic energy of the beam, K_e, at any instant can be expressed as

$$K_e=\frac{1}{2}\int_{-L/2}^{L/2}\left[\rho A\left(\frac{\partial u_0(x,t)}{\partial t}\right)^2+\rho A\left(\frac{\partial w_0(x,t)}{\partial t}\right)^2+\rho I\left(\frac{\partial^2 w_0(x,t)}{\partial x\partial t}\right)^2\right]\mathrm{d}x \tag{10}$$

where ρ is the mass of the beam per unit volume. The eccentric prestress load, T, can be transferred to the gravity center of the cross-section of the beam as an axial prestress load and a couple (see Fig. 1b). In this case, the potential of the external loads and the couples at any instant is given below:

$$V=-P(t)w_0(x_P,t)[c(t-t_1)-c(t-t_2)]+Tu_0(L/2,t)+M_T\frac{\partial w_0(-L/2,t)}{\partial x}-M_T\frac{\partial w_0(L/2,t)}{\partial x} \tag{11a}$$

$$c(t)=\begin{cases}1, & 0\leqslant t\\ 0, & 0>t\end{cases} \tag{11b}$$

$$P(t)=P_0\sin(\Omega t) \tag{11c}$$

$$M_T=Te \tag{11d}$$

where P_0 is the amplitude of the moving harmonic load, Ω the excitation frequency of the moving harmonic load, $c(t)$ the unit step function, t_1 the time when the load $P(t)$ just comes onto the beam (t_1 is considered as zero in this study), t_2 the time when the load $P(t)$ just leaves the beam, e the eccentricity of the prestress load and $x_P(t)$ the location of the moving harmonic load at any instant and expressed as

$$x_P(t)=vt-L/2,\ -L/2\leqslant x_P(t)\leqslant L/2, t_1=0\leqslant t\leqslant t_2=L/v \tag{12}$$

where v is the velocity of the moving harmonic load along the axial direction. The functional of the problem is given below:

$$J=K_e-(U+V) \tag{13}$$

As it is known, Hamilton's principle can be expressed as Lagrange equations when the functions of infinite dimensions can be expressed in terms of generalized coordinates $q_n(t)$. In this situation, when some expressions satisfying kinematic boundary conditions are selected for $w_0(x,t)$ and $u_0(x,t)$, then by using the Lagrange equations, the natural (dynamic) boundary conditions are also satisfied. Therefore, by using the Lagrange equations and by assuming the transverse displacements $w_0(x,t)$ and the longitudinal displacements $u_0(x,t)$ to be representable by a series of admissible functions and by adjusting the coefficients in the series to satisfy the Lagrange equations, approximate solutions are found for the transverse and longitudinal displacements. To apply the Lagrange equations, the displacement functions $w_0(x,t)$ and $u_0(x,t)$ are approximated by the

following series:

$$w_0(x,t)=\sum_{n=1}^{N}A_n(t)x^{n-1} \tag{14a}$$

$$u_0(x,t)=\sum_{n=1}^{N}B_n(t)x^{n-1} \tag{14b}$$

where $A_n(t)$ and $B_n(t)$ are time-dependent generalized coordinates. Kinematic (geometric) boundary conditions of the simply supported beam with one movable support are

$$u_0(x,t)=0 \quad \text{at } x=-L/2, \quad w_0(x,t)=0 \quad \text{at } x=-L/2, L/2 \tag{15}$$

It is seen from Eqs. (14a to b) that kinematic boundary conditions given by Eq. (15) are not satisfied for $w_0(x,t)$ and $u_0(x,t)$. Thus, the constraint conditions of the supports are satisfied by using the Lagrange multipliers. The Lagrange multipliers formulation of the considered problem requires constructing the Lagrangian functional as follows:

$$J^*=J+\beta_1 w_0(-L/2,t)+\beta_2 w_0(L/2,t)+\beta_3 u_0(-L/2,t) \tag{16}$$

In Eq. (16), β_1, β_2 and β_3 quantities are the Lagrange multipliers, which are the support reactions in the considered problem. By introducing the following definitions:

$$q_n=A_n, \quad n=1,2,\ldots,N \tag{17a}$$

$$q_n=B_{n-N}, \quad n=N+1,\ldots,2N \tag{17b}$$

$$q_{2N+1}=\beta_1, q_{2N+2}=\beta_2, q_{2N+3}=\beta_3 \tag{17c}$$

After substituting Eq. (14) into Eq. (16) and then using the Lagrange's equations,

$$\frac{\partial J^*}{\partial q_n}-\frac{\mathrm{d}}{\mathrm{d}t}\left(\frac{\partial J^*}{\partial \dot{q}_n}\right)+Q_D=0, \quad n=1,2,\ldots,2N+3 \tag{18}$$

where Q_D is the generalized damping force that can be obtained from the dissipation function by differentiating D with respect to $\dot{q}_n$

$$Q_D=-\frac{\partial D}{\partial \dot{q}_n}, \quad n=1,2,3,...,2N+3 \tag{19}$$

yields the following two coupled nonlinear systems of equations of motion:

$$\begin{bmatrix} \left[\mathbf{K}_1^L\right]_{N\times N} & [\mathbf{0}]_{N\times N} & \left[\mathbf{K}_6^S\right]_{N\times 3} \\ [\mathbf{0}]_{N\times N} & \left[\mathbf{K}_2^L\right]_{N\times N} & \left[\mathbf{K}_7^S\right]_{N\times 3} \\ \left[\mathbf{K}_8^S\right]_{3\times N} & \left[\mathbf{K}_9^S\right]_{3\times N} & [\mathbf{0}]_{3\times 3} \end{bmatrix} \begin{Bmatrix} \mathbf{A}(t) \\ \mathbf{B}(t) \\ \boldsymbol{\beta}(t) \end{Bmatrix} + \begin{bmatrix} \left[\mathbf{K}_3^{NL}(A(t))\right]_{N\times N} & \left[\mathbf{K}_4^{NL}(A(t))\right]_{N\times N} & [\mathbf{0}]_{N\times 3} \\ \left[K_5^{NL}(A(t))\right]_{N\times N} & [\mathbf{0}]_{N\times N} & [\mathbf{0}]_{N\times 3} \\ [\mathbf{0}]_{3\times N} & [\mathbf{0}]_{3\times N} & [\mathbf{0}]_{3\times 3} \end{bmatrix} \begin{Bmatrix} \mathbf{A}(t) \\ \mathbf{B}(t) \\ \mathbf{0} \end{Bmatrix}$$
$$+\eta \begin{bmatrix} \left[\mathbf{K}_1^L\right]_{N\times N} & [\mathbf{0}]_{N\times N} & [\mathbf{0}]_{N\times 3} \\ [\mathbf{0}]_{N\times N} & \left[\mathbf{K}_2^L\right]_{N\times N} & [\mathbf{0}]_{N\times 3} \\ [\mathbf{0}]_{3\times N} & [\mathbf{0}]_{3\times N} & [\mathbf{0}]_{3\times 3} \end{bmatrix} \begin{Bmatrix} \dot{\mathbf{A}}(t) \\ \dot{\mathbf{B}}(t) \\ \mathbf{0} \end{Bmatrix} + \begin{bmatrix} \left[\mathbf{M}_1^L\right]_{N\times N} & [\mathbf{0}]_{N\times N} & [\mathbf{0}]_{N\times 3} \\ [\mathbf{0}]_{N\times N} & \left[\mathbf{M}_2^L\right]_{N\times N} & [\mathbf{0}]_{N\times 3} \\ [\mathbf{0}]_{3\times N} & [\mathbf{0}]_{3\times N} & [\mathbf{0}]_{3\times 3} \end{bmatrix} \begin{Bmatrix} \ddot{\mathbf{A}}(t) \\ \ddot{\mathbf{B}}(t) \\ \mathbf{0} \end{Bmatrix} = \begin{Bmatrix} \mathbf{f}_1(t) \\ \mathbf{f}_2(t) \\ \mathbf{0} \end{Bmatrix} \tag{20}$$

where $\mathbf{K}_1^L$ is the linear bending stiffness matrix, $\mathbf{K}_2^L$ is the linear axial stiffness matrix, matrices $\mathbf{K}_6^S, \mathbf{K}_7^S, \mathbf{K}_8^S$ and $\mathbf{K}_9^S$ exist due to Lagrange multipliers, $\mathbf{K}_3^{NL}$ is the nonlinear stiffness matrix that is quadratically dependent on the generalized coordinates, both $\mathbf{K}_4^{NL}$ and $\mathbf{K}_5^{NL}$ are the nonlinear stiffness matrices that are linearly dependent on the generalized coordinates, $\mathbf{M}_1$ is the bending mass matrix, $\mathbf{M}_2$ is the axial mass matrix, $\mathbf{f}_1$ is the vector of the generalized load generated by the moving harmonic load and the couple, $\mathbf{f}_2$ is the vector of the generalized load generated by the external prestress load. The equations of motion are solved by using the implicit time

integration method of Newmark-β in conjunction with the Newton–Raphson method, and then the displacements, velocities and accelerations of the beam at the considered point and time are determined for any time t between $0 \leqslant t \leqslant L/v$. Furthermore, for calculating the terms of the stiffness and mass matrices in Eq. (20), the Gaussian quadrature is used.

The equations of motion (20) can be written in a compact matrix form as follows:

$$\mathbf{K}^L\mathbf{q}(t) + \mathbf{K}^{NL}(\mathbf{q}(t))\mathbf{q}(t) + \mathbf{C}\dot{\mathbf{q}}(t) + \mathbf{M}\ddot{\mathbf{q}}(t) = \mathbf{F}(t) \tag{21}$$

where $\mathbf{q}(t) = \{\mathbf{A}(t), \mathbf{B}(t), \boldsymbol{\beta}(t)\}^{\mathrm{T}}$. It is also worth noting at this stage that, when there is no concentrated moving harmonic load on the beam, the beam is at rest and also it is in a bent configuration under the eccentric axial prestress load. In this case, the initial velocities and accelerations of the beam are zero; however, the initial displacements are not zero at time $t = 0$. Therefore, the initial displacements caused by the eccentric prestress load should be calculated from a nonlinear static analysis and must be introduced to the problem at the beginning of the Newmark-β algorithm.

3. Solution of the equations of motion

The time domain equations of motion equation (21) can be solved by using the average acceleration method of Newmark-β in conjunction with an iteration method, such as direct iteration or the Newton–Raphson method. By using the average acceleration method of Newmark-β, the nonlinear differential equations of motion (21) can be reduced to the following set of nonlinear algebraic equations [27]:

$$\hat{\mathbf{K}}(\mathbf{q}_{i+1})\mathbf{q}_{i+1} = \hat{\mathbf{F}}_{i,i+1} \tag{22}$$

where subscript $i+1$ denotes the time $t = t_{i+1}$, $\hat{\mathbf{K}}(\mathbf{q}_{i+1})$ and $\hat{\mathbf{F}}_{i,i+1}$ are the effective stiffness matrix and the effective load vector, which can be expressed as

$$\hat{\mathbf{K}}(\mathbf{q}_{i+1}) = \mathbf{K}^L + \mathbf{K}^{NL}(\mathbf{q}_{i+1}) + a_0\mathbf{M} + a_1\mathbf{C} \tag{23a}$$

$$\hat{\mathbf{F}}_{i,i+1} = \mathbf{F}_{i+1} + \mathbf{M}(a_0\mathbf{q}_i + a_2\dot{\mathbf{q}}_i + a_3\ddot{\mathbf{q}}_i) + \mathbf{C}(a_1\mathbf{q}_i + a_4\dot{\mathbf{q}}_i + a_5\ddot{\mathbf{q}}_i) \tag{23b}$$

where

$$\begin{aligned} &a_0 = \frac{1}{\alpha\Delta t^2},\ \ a_1 = \frac{\delta}{\alpha\Delta t},\ \ a_2 = \frac{1}{\alpha\Delta t}\ \ , a_3 = \frac{1}{2\alpha} - 1\ \ , a_4 = \frac{\delta}{\alpha} - 1 \\ &a_5 = \frac{\Delta t}{2}\left(\frac{\delta}{\alpha} - 2\right),\ \ a_6 = \Delta t(1-\delta),\ \ a_7 = \delta\Delta t,\ \ \delta = 0.5,\ \ \alpha = 0.25 \end{aligned} \tag{24}$$

In order to solve the nonlinear algebraic equations (22), an iterative solution procedure should be used. In this study, the Newton–Raphson method is used to solve the above-mentioned equations. Eq. (22) at any fixed time can be written as follows [27]:

$$\mathbf{R}(\mathbf{q}_{i+1}) \equiv \hat{\mathbf{K}}(\mathbf{q}_{i+1})\mathbf{q}_{i+1} - \hat{\mathbf{F}}_{i,i+1} = \mathbf{0} \tag{25}$$

where $\mathbf{R}$ is the residual vector. By assuming that the solution $\mathbf{q}_{i+1}^{s-1}$ at the $(s-1)$ st iteration is known, the residual vector $\mathbf{R}$ can be expanded in Taylor's series about the known solution $\mathbf{q}_{i+1}^{s-1}$ as follows:

$$\mathbf{R}(\mathbf{q}_{i+1}) = \mathbf{R}(\mathbf{q}_{i+1}^{s-1}) + \left(\frac{\partial\mathbf{R}(\mathbf{q}_{i+1})}{\partial\mathbf{q}_{i+1}}\right)^{s-1} \cdot \delta\mathbf{q}_{i+1} + \cdots = \mathbf{0} \tag{26}$$

Neglecting the terms of order two and higher gives the following equations:

$$\hat{\mathbf{K}}_T(\mathbf{q}_{i+1}^{s-1}) \cdot \delta\mathbf{q}_{i+1} = -\mathbf{R}(\mathbf{q}_{i+1}^{s-1}) = \hat{\mathbf{F}}_{i,i+1} - \hat{\mathbf{K}}(\mathbf{q}_{i+1}^{s-1})\mathbf{q}_{i+1}^{s-1} \tag{27}$$

where $\hat{\mathbf{K}}_T$ is the tangent stiffness matrix, which is defined as follows:

$$\hat{\mathbf{K}}_T(\mathbf{q}_{i+1}^{s-1}) \equiv \left(\frac{\partial\mathbf{R}(\mathbf{q}_{i+1})}{\partial\mathbf{q}_{i+1}}\right)^{s-1} \tag{28}$$

Incremental displacements, $\delta\mathbf{q}_{i+1}$, and the solution at the (s) th iteration, $\mathbf{q}^{s}{}_{i+1}$, can be easily calculated by

$$\delta\mathbf{q}_{i+1} = -\hat{\mathbf{K}}_T^{-1}(\mathbf{q}_{i+1}^{s-1})\mathbf{R}(\mathbf{q}_{i+1}^{s-1}) \tag{29a}$$

$$\mathbf{q}_{i+1}^{s} = \mathbf{q}_{i+1}^{s-1} + \delta\mathbf{q}_{i+1} \tag{29b}$$

This procedure is continued until the difference between two successive solution vectors is less than a selected tolerance criterion in Euclidean norm given by

$$\sqrt{\frac{\sum_{n=1}^{2N+3}\left|q_n^s - q_n^{s-1}\right|^2}{\sum_{n=1}^{2N+3}\left|q_n^s\right|^2}} \leqslant \zeta_{\text{tol}} \tag{30}$$

Once Eq. (22) is solved for the displacements $\mathbf{q}$ at time $t = t_{i+1}$, the new acceleration vector $\ddot{\mathbf{q}}$, and the new velocity vector $\dot{\mathbf{q}}$ at time $t = t_{i+1}$ are computed from the following equations:

$$\ddot{\mathbf{q}}_{i+1} = a_0(\mathbf{q}_{i+1} - \mathbf{q}_i) - a_2\dot{\mathbf{q}}_i - a_3\ddot{\mathbf{q}}_i \tag{31a}$$

$$\dot{\mathbf{q}}_{i+1} = \dot{\mathbf{q}}_i + a_6\ddot{\mathbf{q}}_i + a_7\ddot{\mathbf{q}}_{i+1} \tag{31b}$$

After the displacements $\mathbf{q}_{i+1}$, the accelerations $\ddot{\mathbf{q}}_{i+1}$ and the velocities $\dot{\mathbf{q}}_{i+1}$ are calculated, which correspond to time $t = t_{i+1}$, all these procedures mentioned above are repeated for the next time step. Meanwhile, in general, when solving the nonlinear equations, the initial solution vector is chosen to be zero vector, namely, the first iteration solution corresponds to the linear solution.

4. Numerical results

In numerical results, the nonlinear dynamic responses of an eccentrically prestressed damped simply supported beam are investigated. The dynamic deflections, velocities and accelerations are calculated numerically and presented in figures. The effects of the large deflections, the velocity of the moving harmonic load, the prestress load and the excitation frequency of the moving harmonic load on the dynamic response of the beam are discussed. The obtained results are compared with the results based on the linear beam theory. It is clear that the corresponding linear problem can be solved by making $\mathbf{K}^{NL} = 0$ in Eq. (21). The material properties of the considered beam are as follows: $E = 35\,\text{GPa}$, $\rho A = 1500\,\text{kg/m}$, and other parameters of the beams and the moving load are taken as various values to investigate the above-mentioned effects. Also, the tolerance criterion ζ_{tol} is taken equal to 0.0001 in the numerical calculations.

In Tables 1–2, comparison and numerical convergence studies are performed with various numbers of terms of displacement functions and various time steps by calculating the maximum dynamic deflections at the mid-point of the beam according to both linear and nonlinear beam theory for $P_0 = 1000\,\text{kN}$, $L = 20\,\text{m}$, $b = 0.4\,\text{m}$,

Table 1
Convergence study of number of N for $L = 20\,\text{m}$, $b = 4\,\text{m}$, $h = 0.9\,\text{m}$, $P_0 = 1000\,\text{kN}$, $v = 40\,\text{m/s}$, $T = 0.1T_{\text{cr}}$, $e = 0$, $\Omega = 0$ for 250 time steps

Number of term in the series, N	Maximum deflections at the mid-point of the beam (m)			
	Linear		Nonlinear	
	$\eta = 0$	$\eta = 0.01\,\text{s}$	$\eta = 0$	$\eta = 0.01\,\text{s}$
6	0.331987	0.298285	0.331980	0.286470
8	0.334455	0.300810	0.334421	0.289276
10	0.334727	0.301256	0.334697	0.289762
12	0.334838	0.301394	0.334801	0.289906
14	0.334892	0.301449	0.334812	0.289963
16	0.334916	0.301475	0.334856	0.289984
18	0.334929	0.301488	0.334826	0.290062

Table 2
Convergence study of number of time step for $L = 20\,\text{m}$, $b = 0.4\,\text{m}$, $h = 0.9\,\text{m}$, $P_0 = 1000\,\text{kN}$, $v = 40\,\text{m/s}$, $T = 0.1T_{\text{cr}}$, $e = 0$, $\Omega = 0$, $\eta = 0.01\,\text{s}$, $N = 12$

Number of time step	Maximum deflections at the mid-point of the beam (m)	
	Linear	Nonlinear
50	0.301495	0.290023
100	0.301417	0.289894
250	0.301394	0.289906
500	0.301395	0.289901
1000	0.301396	0.289903

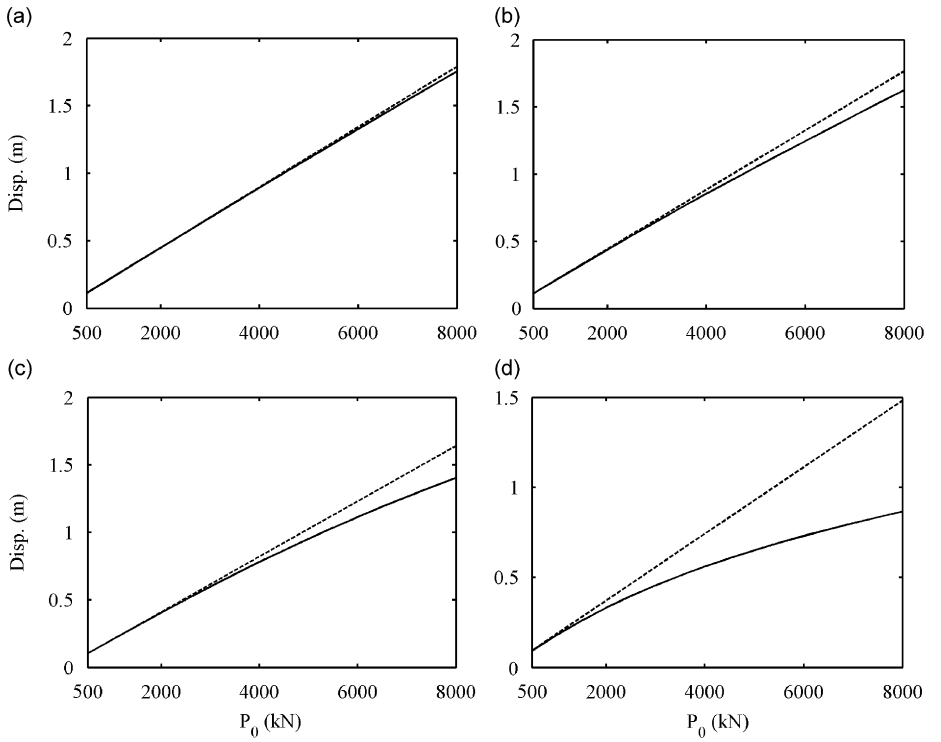

Fig. 2. Effect of internal damping of the beam on the maximum dynamic displacements under the moving load for $L = 20\,\text{m}$, $b = 0.4\,\text{m}$, $h = 0.9\,\text{m}$, $T = 0$, $e = 0$, $\Omega = 0$, $v = 20\,\text{m/s}$, (a) $\eta = 0$, (b) $\eta = 0.001\,\text{s}$, (c) $\eta = 0.01\,\text{s}$, (d) $\eta = 0.1\,\text{s}$; (– – –) linear, (——) nonlinear.

$h = 0.9\,\text{m}$, $T = 0.1T_{\text{cr}}$, where $T_{\text{cr}} = \pi^2 EI/L^2 = 2.0985 \times 10^4\,\text{kN}$ is Euler's buckling load of the considered beam, $e = 0$, $\Omega = 0$, $\eta = 0$, $0.01\,\text{s}$ at the constant velocity $v = 40\,\text{m/s}$. It is seen from Tables 1 to 2 that when more than 12 terms were used, and the number of time steps was taken to be more than 250, the numerical accuracy of the responses was improved only slightly, but the computational load was considerably increased. Moreover, it should be noted that the nonlinear dynamic analysis in the time domain requires iterations in each time step, and takes much more time than a nonlinear static analysis. Therefore, the number of terms in the displacement functions and the number of time steps are set to 12 and 250, respectively, in the subsequent calculations. In the authors' earlier work [17], the higher order polynomial functions were used for expressing the displacement function of the beam, and good agreement was obtained between the exact solution given by Timoshenko and Young [1] and the results given by Kocatürk and Şimşek [17].

Fig. 2 displays the effect of the internal damping on the dynamic behavior of the beam for $L = 20\,\text{m}$, $b = 0.4\,\text{m}$, $h = 0.9\,\text{m}$, $T = 0$, $e = 0$, $v = 20\,\text{m/s}$. For this purpose, linear and nonlinear load-displacement curves are given for the different internal dampings of the beam. In Fig. 2, the dynamic displacements under the moving load are calculated for each value of magnitude of the moving load, which varies from $P_0 = 500\,\text{kN}$ to $P_0 = 8000\,\text{kN}$ with $500\,\text{kN}$ increments, and the maximum of the obtained displacements according to linear and nonlinear theories for each magnitude of the moving load are plotted versus the corresponding P_0 values.

It is known from the different studies in the literature (for example, Ref. [27]), and from the static analysis although it is not shown here, that when one of the supports of the beam is movable in the axial direction, linear and nonlinear static deflections of the beam are equal to each other. In other words, nonlinear behavior does not occur in the static case. However, it is seen from Fig. 2 that nonlinear behavior is observed in the dynamic case even if one of the supports of the beam is movable. Fig. 2a shows that when the internal damping of the beam is zero ($\eta = 0$), the difference between the linear and the nonlinear solutions are very small. The difference in this case stems from taking into account the axial kinetic energy of the beam, as seen from Eq. (10). In the nonlinear case, since the horizontal displacement $u_0(x,t)$ is caused by both axial prestress load T and the bending, axial displacement varies with time and the kinetic energy due to horizontal motion can be taken into account. However, in the linear case, since there is no coupling between the horizontal motion and the transverse motion and since the axial prestress load is constant (independent of time), horizontal motion is independent of time and therefore there is no kinetic energy due to horizontal motion.

On the other hand, the difference between the linear and the nonlinear displacements increases as the internal damping of the beam increases, as shown in Figs. 2b–d. The reason for this behavior can be explained as follows: It is known that the difference between linear and nonlinear displacements of a beam with immovable supports is very significant in both static and dynamic case. The first term in the dissipation function of the beam given by Eq. (9) represents the effect of the internal damping on the axial motion of the

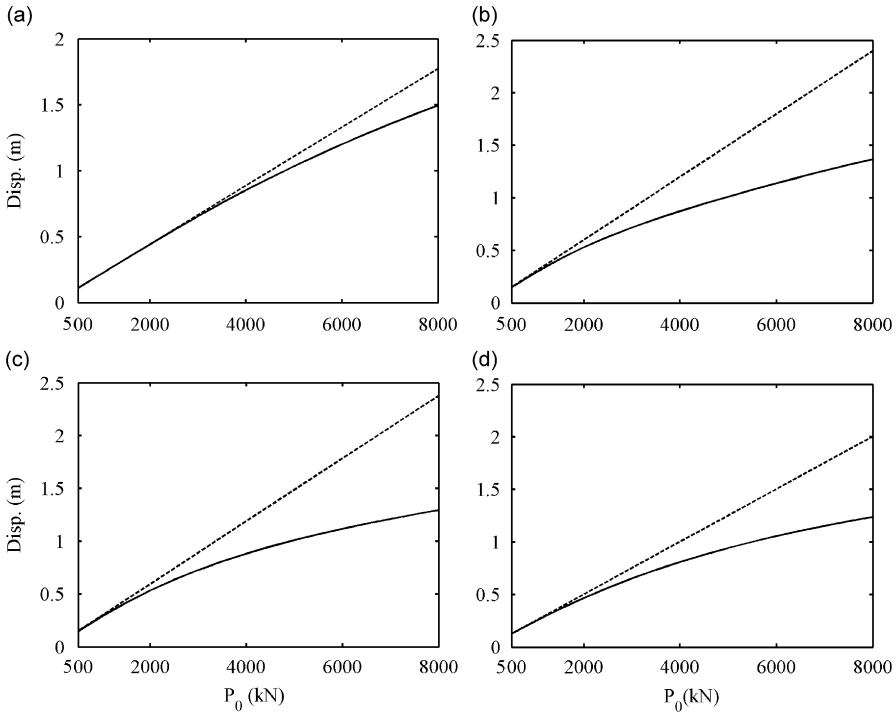

Fig. 3. Effect of the magnitude of the moving load on the maximum dynamic displacements under the moving load for $L = 20\,\text{m}$, $b = 0.4\,\text{m}$, $h = 0.9\,\text{m}$, $T = 0.1T_{cr}$, $e = 0$, $\Omega = 0$, $\eta = 0.01\,\text{s}$: (a) $v = 20\,\text{m/s}$, (b) $v = 40\,\text{m/s}$, (c) $v = 60\,\text{m/s}$, (d) $v = 80\,\text{m/s}$; (– – –) linear, (——) nonlinear.

beam. This effect, like the axial kinetic energy, can be taken into account in the nonlinear case. This effect in the axial direction increases with increase in the internal damping of the beam. Furthermore, for large values of η, the beam with one movable support behaves like a beam with immovable supports.

Fig. 3 shows the effect of the magnitude of the moving load on the maximum dynamic displacements under the moving load ($\Omega = 0$) for $L = 20\,\text{m}$, $b = 0.4\,\text{m}$, $h = 0.9\,\text{m}$, $T = 0.1T_{\text{cr}}$, $e = 0$, $\eta = 0.01\,\text{s}$, and for various values of velocity of the moving load. Fig. 3 reveals that the dynamic deflections of the nonlinear case are smaller than those in the linear case, because the beam is stiffened by the internal normal force N_x generated by the large deflections in the nonlinear case. Also, it is seen from this figure that displacements of the linear and the nonlinear theory are very close to each other until the value of $P_0 = 2000\,\text{kN}$; however, after this value of P_0, displacements deviation between the linear and the nonlinear theory increases for the considered parameters. Furthermore, as seen from this figure, the velocity of the moving load plays an important role on the load-displacement curves and the difference between the two theories is minimum for $v = 20\,\text{m/s}$ for the considered velocities.

The effect of the length of the beam, whose length of span varies from $L = 5$ to $30\,\text{m}$ with $1\,\text{m}$ increments, on the maximum dynamic displacements under the moving load is presented in Fig. 4 for various values of the velocity of the moving load, and for $P_0 = 1000\,\text{kN}$, $b = 0.4\,\text{m}$, $h = 0.9\,\text{m}$, $T = 0.1T_{\text{cr}}$, $e = 0$, $\Omega = 0$, $\eta = 0.01\,\text{s}$. It is seen from Fig. 4 that the difference between the displacements of the two theories increases as the length of the beam increases and decreases as the velocity of the moving load increases, as an expected situation. This situation can be explained as follows: By examining Eq. (4b), it is seen that the magnitude of the internal normal force depends on both the axial and the transverse displacements of the beam. As the length of the beam increases, displacements and the rotations of the cross-sections increase, and then, the effect of the internal normal force increases. Therefore, the beam becomes stiffer with an increase in the internal normal force. It is interesting to note that when the velocity of the moving load is taken as $v = 20\,\text{m/s}$ as seen from Fig. 4a, the difference between the deflections predicted by the two beam models is very small for the beam whose length is up to $L = 25\,\text{m}$. After this value of the beam length, the displacements of the two models

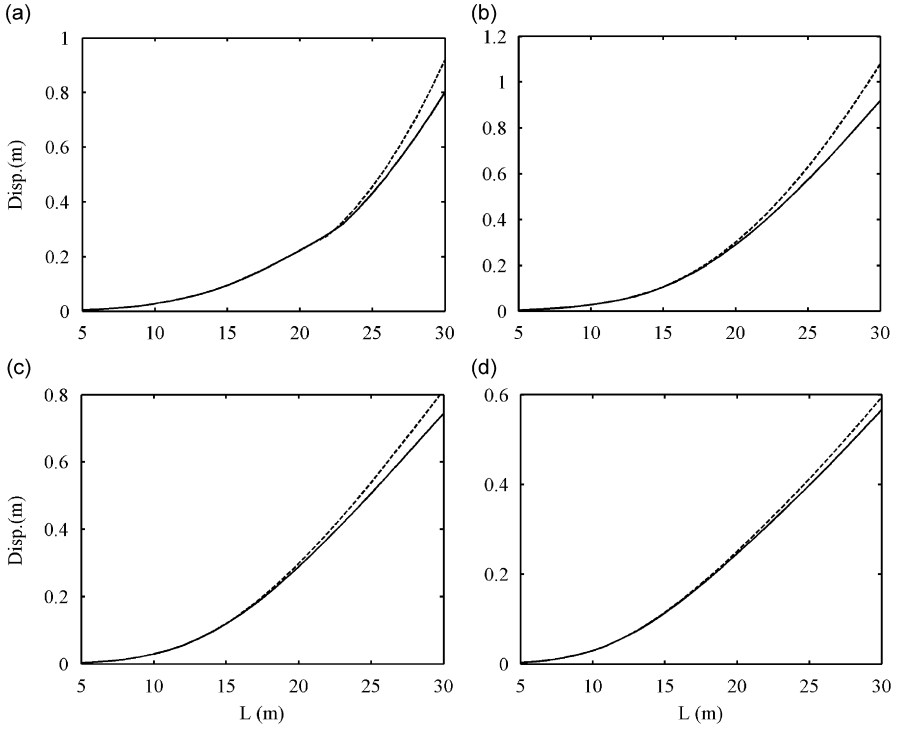

Fig. 4. Effect of the length of the beam on the maximum dynamic displacements under the moving load for $P_0 = 1000\,\text{kN}$, $b = 0.4\,\text{m}$, $h = 0.9\,\text{m}$, $T = 0.1T_{\text{cr}}$, $e = 0$, $\Omega = 0$, $\eta = 0.01\,\text{s}$: (a) $v = 20\,\text{m/s}$, (b) $v = 40\,\text{m/s}$, (c) $v = 60\,\text{m/s}$, (d) $v = 80\,\text{m/s}$; (– – –) linear, (——) nonlinear.

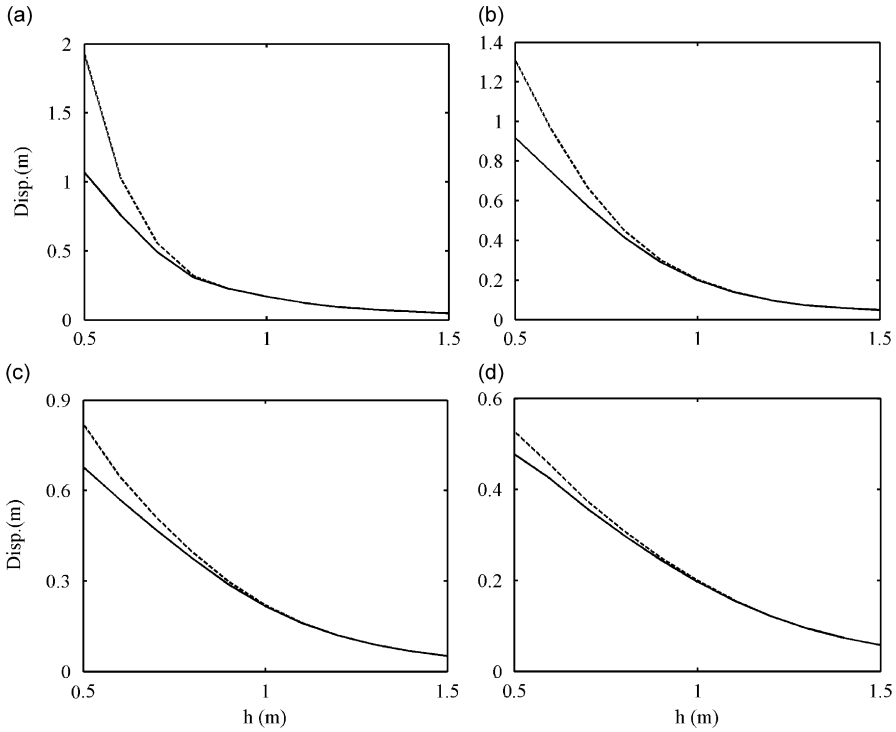

Fig. 5. Effect of the depth of the beam on the maximum dynamic displacements under the moving load for $P_0 = 1000\,\text{kN}$, $L = 20\,\text{m}$, $b = 0.4\,\text{m}$, $T = 0.1T_{\text{cr}}$, $e = 0$, $\Omega = 0$, $\eta = 0.01\,\text{s}$: (a) $v = 20\,\text{m/s}$, (b) $v = 40\,\text{m/s}$, (c) $v = 60\,\text{m/s}$, (d) $v = 80\,\text{m/s}$, (– – –) linear, (——) nonlinear.

deviate from each other. On the other hand, for the values of velocity $v = 40\,\text{m/s}$ and $60\,\text{m/s}$, the displacements deviation of the two theories becomes significant at the lower values of the beam length compared with the values of beam length in the case $v = 20\,\text{m/s}$. Note also that the difference between the two displacement curves is minimum for $v = 80\,\text{m/s}$.

Fig. 5 displays the effect of the depth of the beam on the maximum dynamic displacements under the moving load for various values of the velocity of the moving load and for $P_0 = 1000\,\text{kN}$, $L = 20\,\text{m}$, $b = 0.4\,\text{m}$, $T = 0.1T_{\text{cr}}$, $e = 0$, $\Omega = 0$, $\eta = 0.01\,\text{s}$. As would be expected, as the depth of the beam increases, the deflections of the beam decrease. However, it is known from the linear beam theory that deflections of a beam are inversely proportional to the moment of inertia of the cross-section, and also the moment of inertia is proportional to the third order of the depth of the beam. It is clearly seen from this figure that the difference between the deflections of the linear and the nonlinear model increases as the depth of the beam decreases.

In Fig. 6, the effect of the velocity of the moving load on the maximum absolute value of displacements, velocities and accelerations of the point under the moving load is presented for $P_0 = 1000\,\text{kN}$, $L = 20\,\text{m}$, $b = 0.4\,\text{m}$, $h = 0.9\,\text{m}$, $T = 0.1T_{\text{cr}}$, $e = 0$, $\eta = 0.01\,\text{s}$. In these figures, velocity of the moving load ranges from $v = 1$ to $100\,\text{m/s}$ with $1\,\text{m/s}$ increments. It can be observed from Fig. 6 that the maximum absolute values of the displacements, the velocities and the accelerations of the beam obtained by the linear beam model are greater than those of the nonlinear beam model. It is worth pointing out that the maximum values of the displacements increase with an increase in the velocity of the moving load until a certain value of the velocity of the moving load, and then decrease after this value of the velocity. However, the maximum absolute values of the velocities and the accelerations of the beam show a different character than the character of the displacement curve in the considered velocity range. It is also noticed from this figure that the difference between the maximum deflections of the two beam theories increases for the values of the velocity of the moving load between approximately 25 and $50\,\text{m/s}$, and after approximately $v = 50\,\text{m/s}$, the two deflection curves continuously become close to each other. However, the variation of the velocities and the accelerations

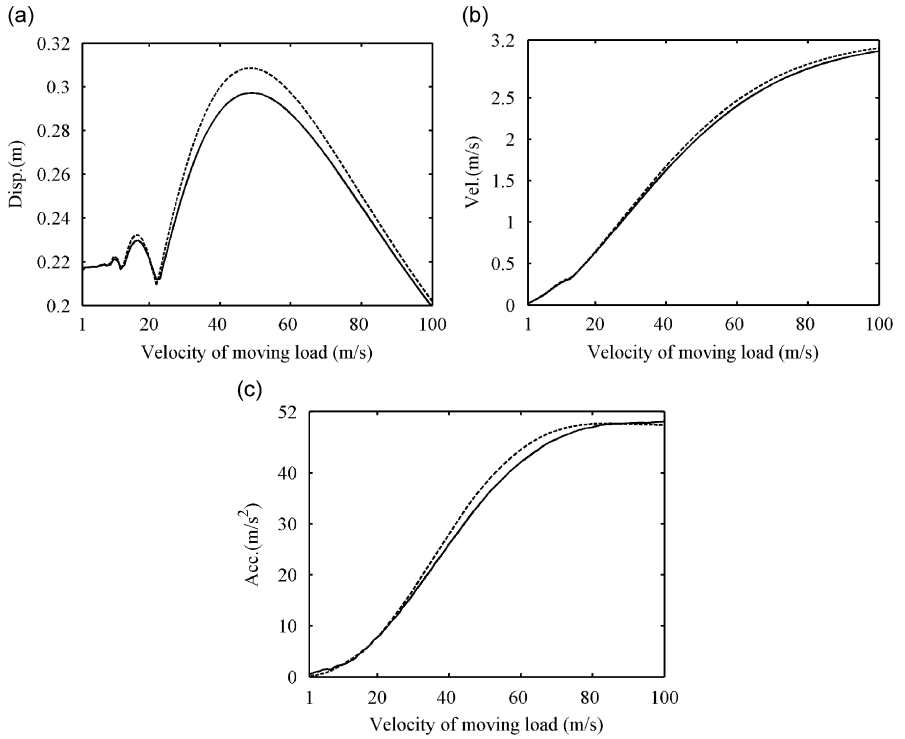

Fig. 6. Effect of the velocity of the moving load on the dynamic responses under the moving load for $P_0 = 1000\,\text{kN}$, $b = 20\,\text{m}$, $b = 0.4\,\text{m}$, $h = 0.9\,\text{m}$, $T = 0.1T_{\text{cr}}$, $e = 0$, $\Omega = 0$, $\eta = 0.01\,\text{s}$, (– – –) linear, (——) nonlinear.

of the beam with the velocity of the moving load show a different behavior from the displacements, as displayed in Figs. 6b and c.

Fig. 7 shows the effect of the axial prestress load with no eccentricity on the displacements, velocities and accelerations under the moving load for $T = 0$, $0.1T_{\text{cr}}$, $0.2T_{\text{cr}}$, $P_0 = 1000\,\text{kN}$, $L = 20\,\text{m}$, $b = 0.4\,\text{m}$, $h = 0.9\,\text{m}$, $\eta = 0.01\,\text{s}$ at the constant velocity $v = 20\,\text{m/s}$. The figures in the first column represent the beam without the prestress load. Fig. 7 indicates that the absolute values of the responses increase as the prestress load increases because of the compression softening effect [10,19]. This effect occurs in the prestressed beams and can be explained as follows. The prestress load reduces the stiffness of the beam, and therefore this effect softens the beam. On the other hand, the internal nonlinear normal force has an opposite effect on the stiffness properties of the beam compared with the prestress load. In other words, for the prestressed beams, the decrease in the stiffness of the beam due to the prestress load is partially compensated by increase in the stiffness of the beam due to the large deflections.

Fig. 8 shows the effect of the eccentricity of the prestress load on the dynamic displacements under the moving load for $P_0 = 1000$, $2000\,\text{kN}$, $L = 20\,\text{m}$, $b = 0.4\,\text{m}$, $h = 0.9\,\text{m}$, $\eta = 0.01\,\text{s}$, $T = 0.1T_{\text{cr}}$. The black and the gray lines represent the linear and the nonlinear responses, respectively. When the prestress load is eccentric, the beam has initial upward deflections before the arrival of the moving load. Therefore, as stated earlier, the initial upward deflections are calculated form a nonlinear static analysis, and must be introduced in Newmark-β algorithm as initial conditions of the problem. It is clearly seen from Fig. 8 that deflections of the beam decrease as the eccentricity of the prestress load increases. This means that the internal tensile stresses due to the moving load can be reduced or completely eliminated by the application of the eccentric prestress load. It is noted in Refs. [17,19] that the total displacements can be obtained by superposing the deflections caused by the moving harmonic load plus the axial prestress load and the deflections due to the bending moments due to the eccentricity of the prestress load. This is true when the superposition principle is valid: namely, when the problem is linear. However, in the present study, the problem is nonlinear and for this

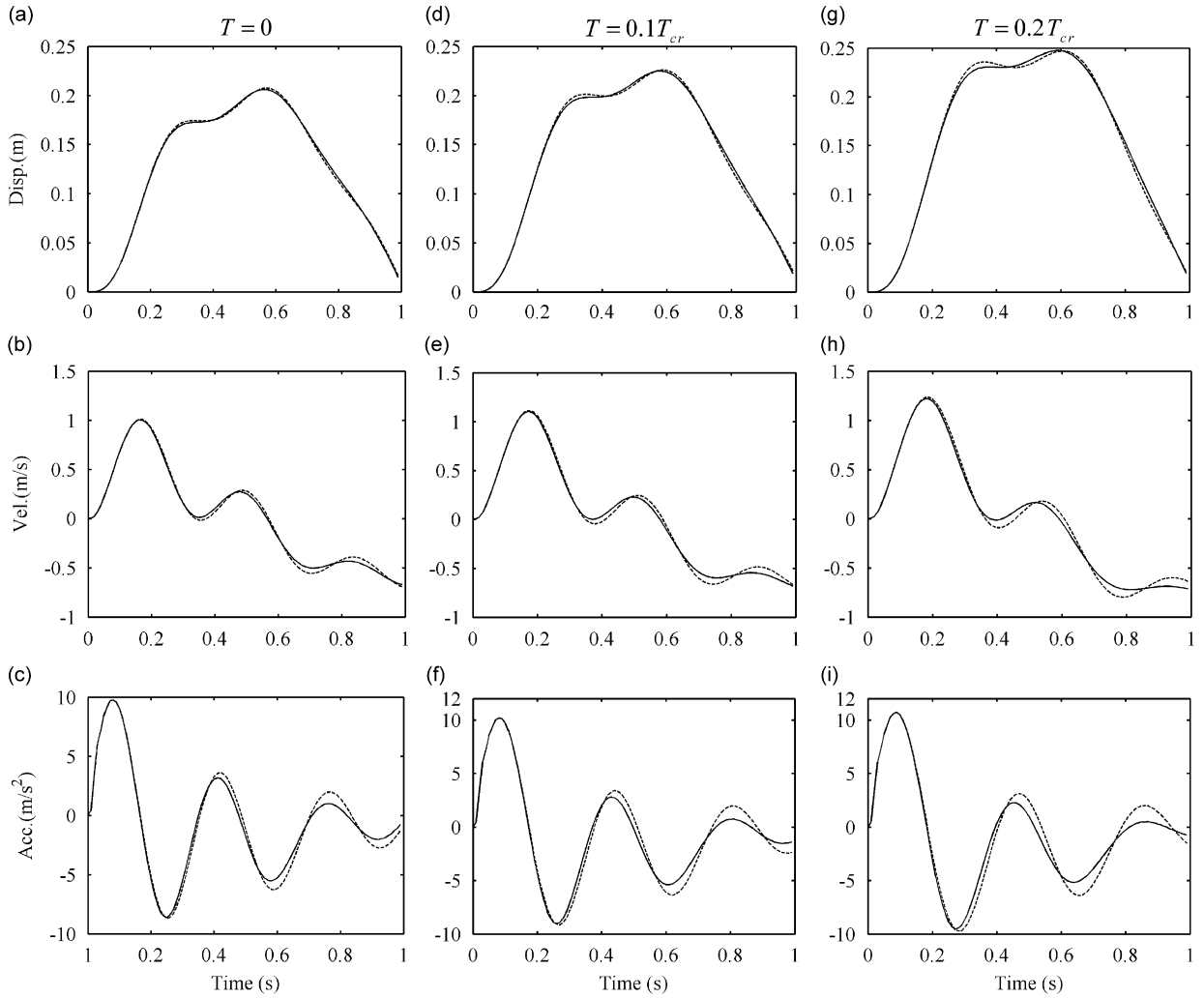

Fig. 7. Effect of the prestress load on the dynamic responses at the mid-point of the beam for $P_0 = 1000\,\text{kN}$, $L = 20\,\text{m}$, $b = 0.4\,\text{m}$, $h = 0.9\,\text{m}$, $v = 20\,\text{m/s}$, $\Omega = 0$, $e = 0$, $\eta = 0.01\,\text{s}$, (– – –) linear, (——) nonlinear.

reason the superposition principle is not valid. Also, the maximum of the obtained displacements and the corresponding velocities are given in Table 3.

Figs. 9–10 display the displacements at the mid-point of the beam for various values of the magnitude of the moving load and for $L = 20$, $30\,\text{m}$, $b = 0.4\,\text{m}$, $h = 0.9\,\text{m}$, $T = 0.1T_{\text{cr}}$, $e = 0$, $\eta = 0.01\,\text{s}$ at the constant velocity $v = 20\,\text{m/s}$. In these figures, the excitation frequency is considered as $\Omega = 0$, 0.50, 0.75, 1.0, 1.25, $1.5\omega_{1l}$ (ω_{1l} is the first linear natural frequency of the beam). The first linear natural frequencies of the beams are obtained as $\omega_{1l} = 17.62603\,\text{rad/s}$ and $\omega_{1l} = 7.83379\,\text{rad/s}$ for $L = 20\,\text{m}$ and $L = 30\,\text{m}$, respectively, from the equation $\omega_{1l} = (\pi/L)^2\sqrt{(EI/\rho A)(1 - T/T_{\text{cr}})}$ [1].

From these figures, it is clear that when $\omega = \omega_{1l}$ for the linear beam model, very large displacements, which are shown by the grey-solid lines, are obtained for the considered beam, as an expected situation. Inspection of Figs. 9a and 10a shows that the linear and the nonlinear responses almost coincide with each other for the small values of the magnitude of the moving load. However, with increase in the value of P_0, the difference between the two solutions becomes significant as seen from Figs. 9c and 10c. It should be noted at this stage that nonlinear natural frequencies vary with the vibration amplitude of the deflection of a beam, and are different from linear frequencies that are independent of the amplitude of the vibration. The cause that makes the nonlinear frequencies change with the amplitude of the vibration is the variation in the stiffness of the

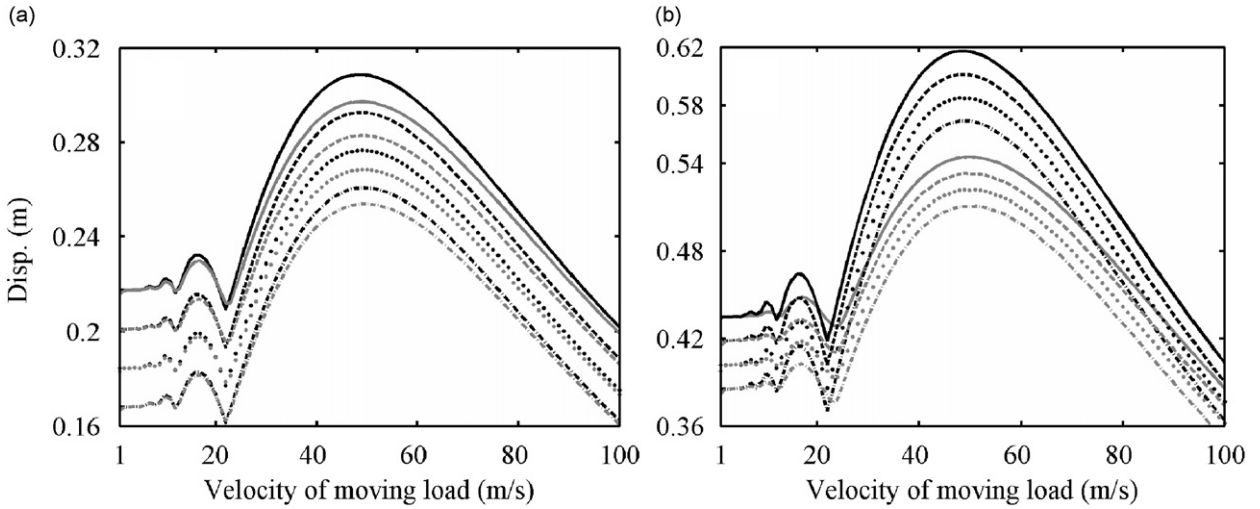

Fig. 8. Effect of the eccentricity of the prestress load on the dynamic displacements under the moving load for $L = 20\,\text{m}$, $b = 0.4\,\text{m}$, $h = 0.9\,\text{m}$, $T = 0.1T_{cr}$, $\Omega = 0$, $\eta = 0.01\,\text{s}$: (a) $P_0 = 1000\,\text{kN}$, (b) $P_0 = 2000\,\text{kN}$, (——) $e = 0$, (– – –) $e = 0.12\,\text{m}$, (· · · · · · · ·) $e = 0.24\,\text{m}$, (– · – · –) $e = 0.36\,\text{m}$; (——) linear, (———) nonlinear.

Table 3
Maximum deflections under the moving load and the corresponding velocities for Fig. 8

P_0 (kN)	e (m)	Max. w (m)		v (m/s)	
		Linear	Nonlinear	Linear	Nonlinear
1000	0	0.308642	0.297261	49	49
	0.12	0.292621	0.282931	49	49
	0.24	0.276605	0.268473	49	49
	0.36	0.26063	0.253878	49	50
2000	0	0.617285	0.544385	49	50
	0.12	0.601264	0.533412	49	50
	0.24	0.585243	0.522282	49	50
	0.36	0.569222	0.511007	49	50

beam with the displacements. Further, the experimental and the theoretical studies in the literature show that nonlinear frequencies increase with increasing vibration amplitude of the beam.

It is seen from Figs. 9 to 10 that increase in the load frequency increases the difference between the displacements of the linear and the nonlinear beam theories significantly until the load frequency values that are close to the first natural frequency of the system. After these frequency values that are close to the first natural frequency of the system, the difference between the two theories becomes small. Namely, increase in the load frequency causes decrease in the difference of the results of the two theories. Also, as the length of the beam increases, while the other parameters remain the same, the displacements of the beam increase, and therefore, as an expected result, increase in the length of the beam increases the difference between the linear and the nonlinear displacements.

Moreover, the numerical calculations for the various values of the eccentricity are made for $e = 0$, 0.12, 0.24, 0.36 m for the parameters used for Figs. 9 and 10, and it is seen that for the considered parameters of the beam, in the considered range of the eccentricity, the eccentricity of the prestress load does not affect the results significantly. Therefore, it is concluded that to give the related figures for various eccentricity makes no sense.

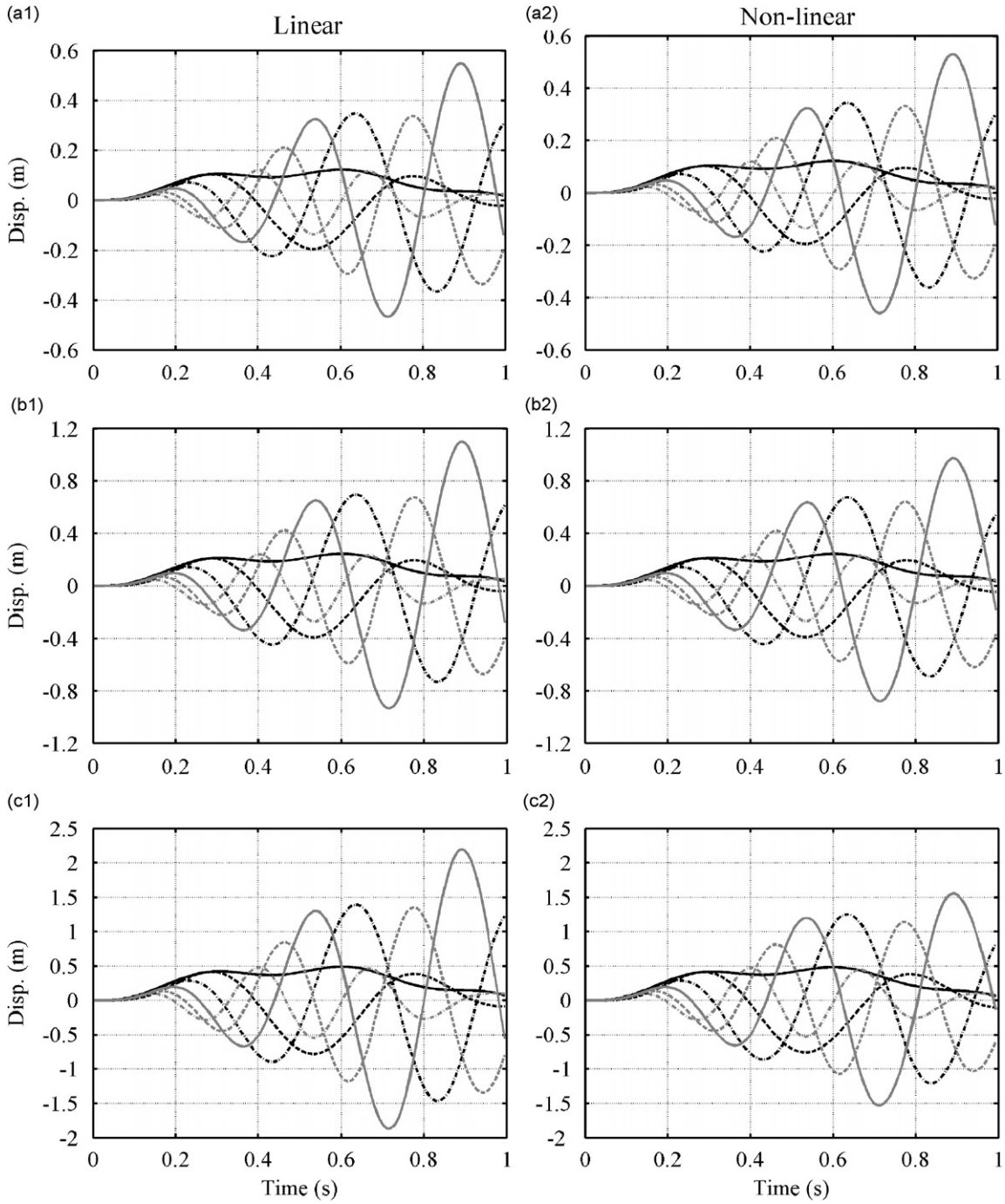

Fig. 9. Displacements at the mid-point of the beam, $L = 20\,\text{m}$, $b = 0.4\,\text{m}$, $h = 0.9\,\text{m}$, $v = 20\,\text{m/s}$, $T = 0.1T_{cr}$, $e = 0$, $\eta = 0.001\,\text{s}$, (a1–a2) $P_0 = 500\,\text{kN}$ (b1–b2) $P_0 = 1000\,\text{kN}$ (c1–c2) $P_0 = 2000\,\text{kN}$, (——) $\Omega = 0$, (– – –) $\Omega = 0.5\omega_{1l}$, (–·–·–) $\Omega = 0.75\omega_1$, (———), $\Omega = \omega_{1l}$, (— — —), $\Omega = 1.25\omega_{1l}$, (— · — · —), $\Omega = 1.5\omega_{1l}$.

5. Conclusions

The dynamic response of an eccentrically prestressed beam subjected to a concentrated moving harmonic load has been studied within the framework of the Euler–Bernoulli beam theory by taking into account the

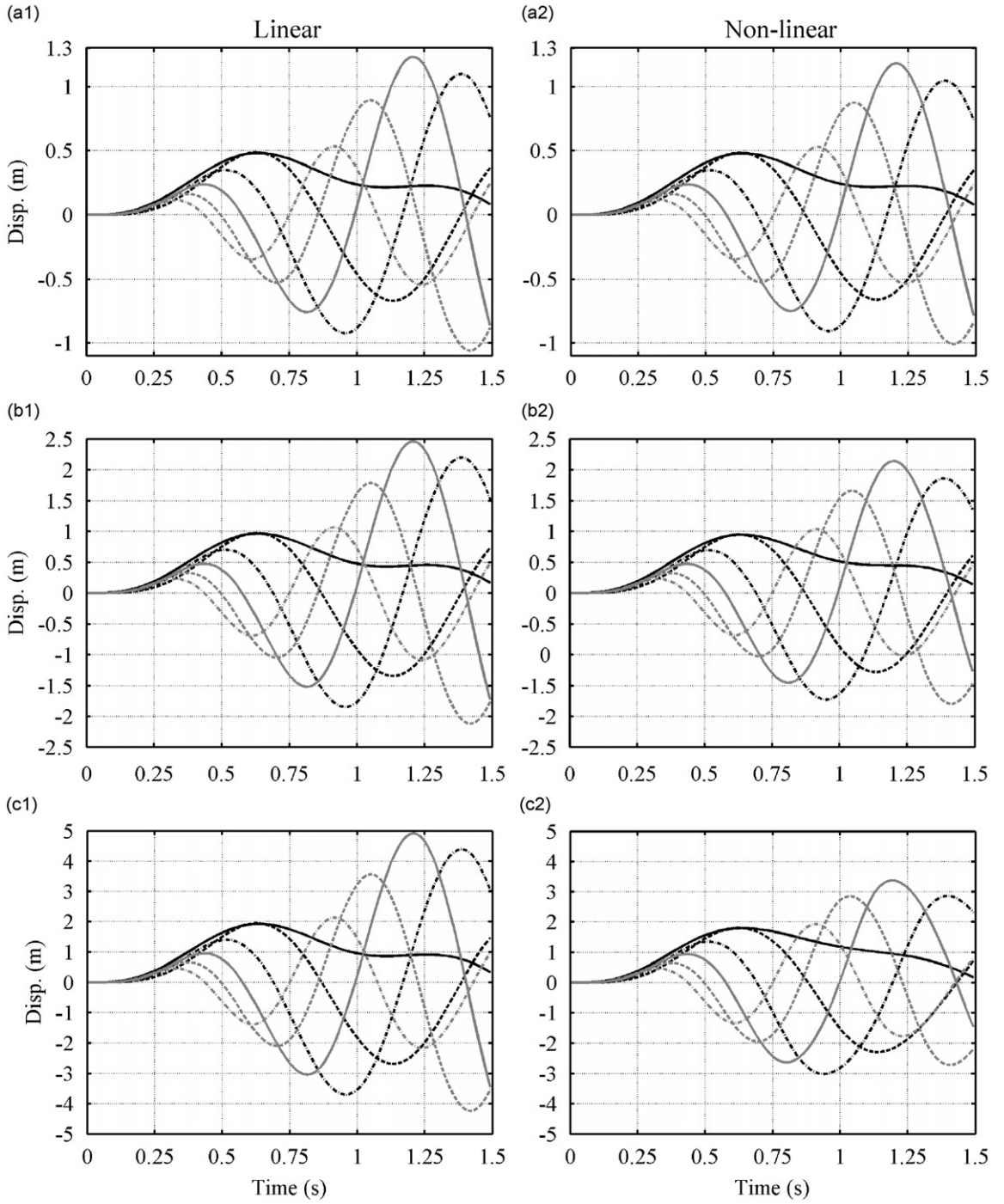

Fig. 10. Displacements at the mid-point of the beam, $L = 30\,\text{m}$, $b = 0.4\,\text{m}$, $h = 0.9\,\text{m}$, $v = 20\,\text{m/s}$, $T = 0.1T_{\text{cr}}$, $e = 0$, $\eta = 0.001\,\text{s}$, (a1–a2) $P_0 = 500\,\text{kN}$ (b1–b2) $P_0 = 1000\,\text{kN}$ (c1–c2) $P_0 = 2000\,\text{kN}$, (——) $\Omega = 0$, (– – –) $\Omega = 0.5\omega_{1l}$, (–·–·–) $\Omega = 0.75\omega_{1l}$, (———), $\Omega = \omega_{1l}$, (— — —), $\Omega = 1.25\omega_{1l}$, (— • — • —), $\Omega = 1.5\omega_{1l}$.

effect of the geometric nonlinearity. The rotary inertia, axial displacement and axial inertia are included in the formulation. The nonlinear equations of motion are derived by using Lagrange's equations, and they are solved by using the implicit time integration method of Newmark-β in conjunction with the Newton–Raphson

method. The effects of the large deflections, the internal damping of the beam, the velocity of the moving harmonic load, the prestress load, the eccentricity of the prestress load and the excitation frequency on the dynamic response of the beam are investigated. The comparison and the convergence studies are performed. It is observed from the investigations that the above-mentioned effects play very important roles in the dynamic behavior of the beam.

Acknowledgments

This work forms a part of the Ph.D. Thesis, which was submitted by the first author to Institute of Science and Technology of Yıldız Technical University, İstanbul.

References

[1] S. Timoshenko, D.H. Young, *Vibration Problems in Engineering*, Van Nostrand Company, New York, 1955.
[2] L. Fryba, *Vibration of Solids and Structures under Moving Loads*, Noordhoff International, Groningen, The Netherlands, 1972.
[3] Y.H. Lin, W. Trethewey, Finite element analysis of elastic beams subjected to moving dynamic loads, *Journal of Sound and Vibration* 136 (1990) 323–342.
[4] H.P. Lee, Dynamic response of a beam with intermediate point constraints subject to a moving load, *Journal of Sound and Vibration* 171 (1994) 361–368.
[5] K. Henchi, K.M. Fafard, G. Dhatt, M. Talbot, Dynamic behavior of multi-span beams under moving loads, *Journal of Sound and Vibration* 199 (1997) 33–50.
[6] R.T. Wang, Vibration of multi-span Timoshenko beams to a moving force, *Journal of Sound and Vibration* 207 (1997) 731–742.
[7] D.Y. Zheng, Y.K. Cheung, F.T.K. Au, Y.S. Cheng, Vibration of multi-span non-uniform beams under moving loads by using modified beam vibration functions, *Journal of Sound and Vibration* 212 (1998) 455–467.
[8] X.Q. Zhu, S.S. Law, Moving force identification on multi-span continuous bridge, *Journal of Sound and Vibration* 228 (1999) 377–396.
[9] T.H.T. Chan, S.S. Law, T.H. Yung, Moving force identification using an existing prestressed concrete bridge, *Engineering Structures* 22 (2000) 1261–1270.
[10] T.H.T. Chan, T.H. Yung, A theoretical study of force identification using prestressed concrete bridges, *Engineering Structures* 23 (2000) 1529–1537.
[11] M. Abu-Hilal, M. Mohsen, Vibration of beams with general boundary conditions due to moving harmonic load, *Journal of Sound and Vibration* 232 (2000) 703–717.
[12] X.Q. Zhu, S.S. Law, Precise time-step integration for the dynamic response of a continuous beam under moving loads, *Journal of Sound and Vibration* 240 (2000) 962–970.
[13] Y.H. Chen, Y.H. Huang, C.T. Shih, Response of an infinite Timoshenko beam on a viscoelastic foundation to a harmonic moving load, *Journal of Sound and Vibration* 241 (2001) 809–824.
[14] G.T. Michaltsos, Dynamic behaviour of a single-span beam subjected to loads moving with variable speeds, *Journal of Sound and Vibration* 258 (2002) 359–372.
[15] Y.A. Dugush, M. Eisenberger, Vibrations of non-uniform continuous beams under moving loads, *Journal of Sound and Vibration* 254 (2002) 911–926.
[16] M. Abu-Hilal, Vibration of beams with general boundary conditions due to a moving random load, *Archive of Applied Mechanics* 72 (2003) 637–650.
[17] T. Kocatürk, M. Şimşek, Vibration of viscoelastic beams subjected to an eccentric compressive force and a concentrated moving harmonic force, *Journal of Sound and Vibration* 291 (2006) 302–322.
[18] T. Kocatürk, M. Şimşek, Dynamic analysis of eccentrically prestressed viscoelastic Timoshenko beams under a moving harmonic load, *Computers and Structures* 84 (2006) 2113–2127.
[19] M. Şimşek, T. Kocatürk, Dynamic analysis of an eccentrically prestressed damped beam under a moving harmonic force using higher order shear deformation theory, *Journal of Structural Engineering—ASCE* 133 (2007) 1733–1741.
[20] J. Hino, T. Yoshimura, N. Ananthanarayana, Vibration analysis of non-linear beams subjected to a moving load using the finite element method, *Journal of Sound and Vibration* 100 (1985) 477–491.
[21] T. Yoshimura, J. Hino, N. Ananthanarayana, Vibration analysis of non-linear beam subjected to moving loads by using the Galerkin method, *Journal of Sound and Vibration* 104 (1986) 179–186.
[22] T. Yoshimura, J. Hino, T. Kamata, N. Ananthanarayana, Random vibration of a non-linear beam subjected to a moving load by a finite element analysis, *Journal of Sound and Vibration* 122 (1988) 317–329.
[23] T.P. Chang, Y.N. Liu, Dynamic finite element analysis of a non-linear beam subjected to a moving load, *International Journal of Solids and Structures* 33 (1996) 1673–1688.
[24] X. Xu, W. Xu, J. Genin, A non-linear moving mass problem, *Journal of Sound and Vibration* 204 (1997) 495–504.

[25] R.T. Wang, T.H. Chou, Non-linear vibration of Timoshenko beam due to a moving force and the weight of beam, *Journal of Sound and Vibration* 218 (1998) 117–1131.
[26] A.N. Yanmeni Wayou, R. Tchoukuegno, P. Woafo, Non-linear dynamics of an elastic beam under moving loads, *Journal of Sound and Vibration* 273 (2004) 1101–1108.
[27] J.N. Reddy, *An Introduction to Nonlinear Finite Element Analysis*, Oxford University Press, Oxford, 2004.
[28] N.M. Newmark, A method of computation for structural dynamics, *Engineering Mechanics Division—ASCE* 85 (1959) 67–94.